

# UNIMAP: UNIVERSAL SMILES-GRAPH REPRESENTATION LEARNING

Shikun Feng<sup>1</sup> Lixin Yang<sup>2</sup> Weiyang Ma<sup>1</sup> Yanyan Lan<sup>1†</sup>

<sup>1</sup>Institute for AI Industry Research, Tsinghua University

<sup>2</sup>Renmin University of China

## ABSTRACT

Molecular representation learning is fundamental for many drug related applications. Most existing molecular pre-training models are limited in using single molecular modality, either SMILES or graph representation. To effectively leverage both modalities, we argue that it is critical to capture the fine-grained ‘semantics’ between SMILES and graph, because subtle sequence/graph differences may lead to contrary molecular properties. In this paper, we propose a universal SMILE-graph representation learning model, namely UniMAP\*. Firstly, an embedding layer is employed to obtain the token and node/edge representation in SMILES and graph, respectively. A multi-layer Transformer is then utilized to conduct deep cross-modality fusion. Specially, four kinds of pre-training tasks are designed for UniMAP, including Multi-Level Cross-Modality Masking (CMM), SMILES-Graph Matching (SGM), Fragment-Level Alignment (FLA), and Domain Knowledge Learning (DKL). In this way, both global (i.e. SGM and DKL) and local (i.e. CMM and FLA) alignments are integrated to achieve comprehensive cross-modality fusion. We evaluate UniMAP on various downstream tasks, i.e. molecular property prediction, drug-target affinity prediction and drug-drug interaction. Experimental results show that UniMAP outperforms current state-of-the-art pre-training methods. We also visualize the learned representations to demonstrate the effectiveness of multi-modality integration.

## 1 INTRODUCTION

Machine learning has been applied to a wide range of tasks in cheminformatics and bioinformatics, including molecular property prediction (Wu et al., 2018), molecular generation (Polykovskiy et al., 2020), and virtual screening (Kimber et al., 2021). Due to the insufficiency of labeled data and engineered features, representation learning becomes an increasingly important tool in replacement of conventional methods, such as manually designed fingerprints (Morgan, 1965).

Inspired by the success of pre-training and fine-tuning paradigm, pre-trained models on molecular data have demonstrated promising results. According to data formats, these models can be mainly classified to two categories, SMILES based and graph based methods. SMILES based methods, taking the SMILES (Weininger, 1988) string as input, have been facilitated by various sequence modeling methods in NLP such as masked language modeling (MLM) (Chithrananda et al., 2020) and auto-encoder (Honda et al., 2019). Despite their ease of use, such methods treat molecules as 1D sequences and may fail to capture the geometric structure of a molecule (Rong et al., 2020). While graph based methods, taking the molecular graph as input, mainly leverage graph level self-supervised training, such as atom/edge/subgraph masking (Hu et al., 2019) and contrastive learning (Wang et al., 2022b;a). These methods directly utilize graph to represent the 2D structure, but may be limited by the over-smoothing (Chen et al., 2020a) and over-squashing (Topping et al., 2022) problems of graph neural networks (GNN).

Given these limitations, a natural idea is to combine SMILES string and molecular graph into one model to enjoy the merits of both approaches. Recently, MOCO (Zhu et al., 2022) designs

<sup>†</sup>Correspondence to lanyanyan@air.tsinghua.edu.cn

\*The code is released publicly at <https://github.com/fengshikun/UniMAP>

a two-stream model to fuse SMILES and graph. Specifically, SMILES and graph are treated as two molecular views, in which a Transformer (Vaswani et al., 2017) branch and a GNN branch are used to obtain their representations, respectively. Then a consistency loss is conducted on the two molecular-level representations for pre-training.

We argue that the above global level alignment cannot well model the correspondence between SMILES and graph. Firstly, SMILES, as a language representation, provides detailed descriptions of a molecular graph, including atoms, bonds, rings, branching, stereochemistry, and isotope. As a result, the global level alignment as in MOCO may fail to recognize the subtle difference between molecules, and cause severe prediction error. For example, substitution of a single fragment will lead to drug deactivation in virtual screening. We give two example pairs in Figure 1 for demonstration. In Pair 1, we replace 4-methylbenzyl (SMILES:c1ccc(C)cc1) with 2-hydroxymethylfuran (SMILES:c1ccc(CO)o1), and find that the modified compound no longer inhibits HIV replication. Similarly in Pair 2, if we replace just a single atom, i.e. thiol (SMILES: S) to chloride (SMILES: Cl), the same result is observed. We have tested previous models on this specific case, including representative SMILES based method ChemBERTa (Chithrananda et al., 2020) and graph based method GROVER (Rong et al., 2020). The similarity results of both ChemBERTa and GROVER are larger than 0.8 for each pair, while UniMAP obtains much smaller similarity results, i.e. 0.55 for Pair 1 and 0.74 for Pair 2. Since the code of MOCO is not released and we cannot reproduce the results in their paper, we do not report the MOCO results on this case. However, given the similarity results from ChemBERTa and GROVER, a single consistency loss will not introduce much difference.

From the above analysis, it is critical to capture the fine-grained ‘semantics’ between SMILES and graph. To this end, we adopt fragments as the basic unit, and propose a multi-modality molecular pre-training model UniMAP, to obtain the UNiVersal sMiles-grAPh representation for molecule. Fragments play a very important role in computational pharmaceutical research (Liu et al., 2017; Lewell et al., 1998). Specifically, molecular fragments are chemically feasible substructures, which to some extent largely determine molecular biological activities and even influence the affinity between a molecule and its target proteins. Therefore, fragments are meaningful substructures to reflect the fine-grained ‘semantics’ between SMILES and graph.

To extract meaningful fragments, we first employ BRICS algorithm (Degen et al., 2008), to split a molecular graph to different fragments. Then we design a SMILES-graph fragment decomposition algorithm to obtain the corresponding SMILES fragment for each graph fragment. In this way, we could use an embedding layer to obtain both token and fragment representations for a molecule, which act as heterogenous inputs to facilitate different pre-training tasks. Afterward, a shared Transformer backbone is utilized to conduct deep cross-modality fusion, and output the unified representation for fine-tuning. As for pre-training, besides two molecular-level tasks including SMILES-Graph Matching (SGM) and Domain Knowledge Learning (DKL), we introduce two novel fragment-level tasks to achieve fine-grained cross-modality interactions, i.e. Multi-Level Cross-Modality Masking (CMM) and Fragment-Level Alignment (FLA). Using both fragments and tokens as masking units, CMM forces the model to acquire both single- and cross-modality information, while FLA uses the fragment embeddings from different modalities as the contrastive learning unit to capture fine-grained cross-modality semantics. In this way, UniMAP learns a better molecular representation by leveraging the fine-grained semantic correlation between SMILES and graph.

We pre-train UniMAP on 10 million molecules from Pubchem (Kim et al., 2019), and then fine-tune the pre-trained model on various downstream tasks. We achieve state-of-the-art results on molecular property prediction tasks from MoleculeNet and outperform existing methods on drug-target affinity prediction and drug-drug interaction task. Our further visualization analysis shows typical fragment alignment patterns and clear embedding clusters, demonstrating the ability of UniMAP to capture both fragment-level and molecular-level ‘semantics’.

Our main contributions are three folds:

- We propose UniMAP, the first single-stream multi-modality molecular representation learning method to leverage both SMILES and graph representation;
- We design both molecular-level (SGM and DKL) and fragment-level (CMM and FLA) pre-training tasks to achieve deep cross-modality fusion in UniMAP;

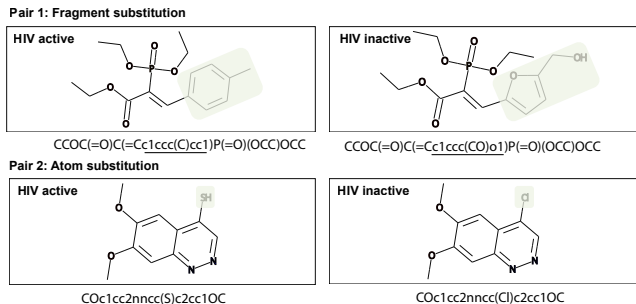


Figure 1: Two examples to demonstrate that substitution of a single fragment will lead to opposite properties in HIV dataset from MoleculeNet (Wu et al., 2018). Specifically, the green parts in graph and the underlined parts in SMILES indicate the differences between two molecules. A molecule is labeled as HIV active if it can inhibit HIV replication and HIV inactive otherwise.

- We conduct experiments on downstream tasks including molecular property prediction, drug-target affinity prediction and drug-drug interaction prediction, and demonstrate promising results of UniMAP.

## 2 RELATED WORK

Here we briefly introduce some typical molecular representation learning methods, including SMILES based methods, graph based methods, 3D based methods and hybrid methods using multiple kinds of molecular input.

### 2.1 SMILES BASED METHODS

Due to the sequential format of a SMILES string, NLP based pre-training methods (Devlin et al., 2019; Liu et al., 2019; Zhu et al., 2020), have been recently applied to SMILES and achieved competitive results. For example, SMILES-BERT (Wang et al., 2019) and ChemBERTa (Chithrananda et al., 2020) use BERT and RoBERTa as backbone to conduct MLM on SMILES, respectively. While SMILES Transformer (Honda et al., 2019) and X-MOL (Xue et al., 2021) leverage an encoder-decoder architecture to learn the representation by SMILES generation. Owing to the success of large scale language models, these models have the ability to utilize large scale molecular data for pre-training, e.g. 1.1 billion molecules in X-MOL. However, previous work (Rong et al., 2020) have shown that these methods are limited in capturing molecular structure.

### 2.2 GRAPH BASED METHODS

In general, graph based pre-training methods can be mainly classified into three categories: generative, predictive and contrastive methods. The objective of generative methods is to reconstruct the original molecular graph or generate 1D sequence by 2D graph. For example, MGSSL (Zhang et al., 2021) generates the motif tree of molecules using a pre-defined motif vocabulary, PanGu (Lin et al., 2022) takes 2D graph as input to generate 1D Self-Referencing Embedded Strings (SELFIES) (Krenn et al., 2020) via a conditional variational autoencoder. Predictive methods construct context based on the graph structure, and adopt context aware masking for self-supervised learning. For example in Hu et al. (2019); Rong et al. (2020), they define neighbors in a graph as context, and use corresponding context on molecular graph to predict the masked atoms/edges/motifs. While contrastive methods mainly apply contrastive learning on molecular graph. For example, MolCLR (Wang et al., 2022b) and iMolCLR (Wang et al., 2022a) firstly transform graphs by atom/edge/sub-graph masking to construct positive and negative pairs, and utilize a contrastive loss. Besides, some other works use chemical knowledge for data augmentation in contrastive learning, e.g. KCL (Fang et al., 2022b) and MPG (Li et al., 2021b).

### 2.3 3D BASED METHODS

Recently, several methods have been proposed to pre-train on 3D molecular conformations. For example, GraphMVP (Liu et al., 2022), 3D-Infomax (Stärk et al., 2022), and GeomGCL (Li et al., 2022) adopt contrastive or generative learning framework between 2D graph and 3D input, to leverage 3D information to enhance the representations of 2D graph. GEM (Fang et al., 2022a) develops a geometry learning task to predict the atom distances and angles from 3D conformation. Besides, some works such as Uni-Mol (Zhou et al., 2022), Transformer-M (Luo et al., 2022) and 3D-EMGP (Jiao et al., 2022), propose to use 3D denoising methods to directly obtain the 3D molecular representation, and has achieved remarkable performances due to the proven equivalence between 3D denoising objective and learning a force field (Zaidi et al., 2022). To our understanding, representation using 3D data is definitely a promising direction. Still, 3D data are relatively not so large as compared with 1D or 2D data. Besides, what objective is the best to reflect the characteristics of 3D conformation is not clear yet. Therefore, how to learn a reliable 3D conformation representation remains a challenging problem.

### 2.4 HYBRID METHODS

Since a molecule can be represented as multiple forms, e.g. SMILES, 2D graph, 3D conformations, IUPAC (Panico et al., 1993), and cell-based microscopy images, some hybrid methods have been proposed to combine different forms to learn a unified representation. DMP (Zhu et al., 2021), MM-Deacon (Guo et al., 2022) and CLOOME (Sanchez-Fernandez et al., 2022) combine 2D graph with SMILES, IUPAC with SMILES, and cell-based microscopy image with 2D graph, respectively. Moreover, MOCO (Zhu et al., 2022) takes advantage of four molecular data forms contain SMILES, 2D graph, 3D conformations and Morgan fingerprints for pre-training. However, these methods all use a two-stream or multi-stream model architecture, in which a separate encoder is first employed to obtain the representation of each data form, and then these representations are aligned with further loss, such as view consistency (in MOCO), multi-lingual contrastive alignment (in MM-Deacon), and InfoLOOB contrastive loss (in CLOOME). These two-stream models are good at learning the representation of each form, but miss the rich alignment information between different forms.

### 2.5 RELATIONS OF UNIMAP WITH PREVIOUS WORK

Our work presents the first single-stream hybrid model, to adapt to the corresponding relation between SMILES and graph. The basic idea of fine-grained alignment, though designed for SMILES and graph in our work, is also valid for combining other data forms, such as IUPAC and cell-based microscopy images. In future, we will investigate how to design a general framework to integrate different data forms.

Our work is also highly inspired by some recent vision-language multi-modality research, which can be categorized to two-stream and single-stream methods. According to the analysis in WenLanHuo et al. (2021) and SemVLPLi et al. (2021a), two-stream methods such as CLIPRadford et al. (2021), ALIGNJia et al. (2021) and WenLan are good at capturing weak correlation between vision and language, while single-stream methods such as OscarLi et al. (2020b) and UinterChen et al. (2020b) are more suitable to model strong correlation. From our study, SMILES and graph have a typical strong correlation, i.e. SMILES provides detailed description of graph, just like the strong correlation between image and language in image caption task. That is why we think a single-stream architecture is better for fusion between different data forms of a molecule.

## 3 METHOD

In this section, we introduce our proposed UniMAP, as shown in Figure 2, including an input embedding layer, a Transformer encoder, and four pre-training tasks.

### 3.1 EMBEDDING LAYER

The embedding layer is designed to map the given SMILES and graph of a molecule to embeddings for further computation. For an input SMILES, we adopt a regex based tokenizer from

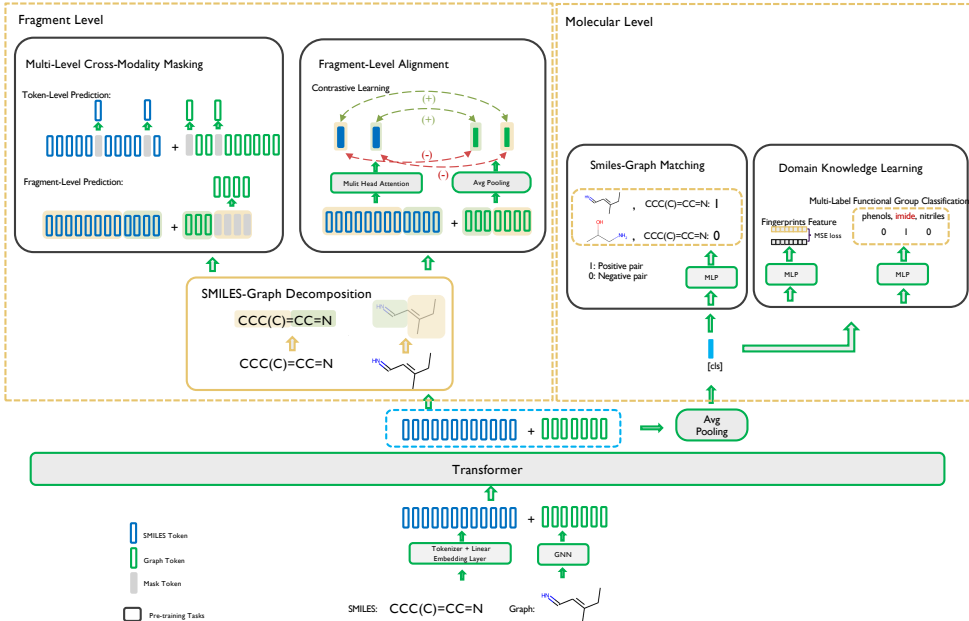


Figure 2: Overview of UniMAP. SMILES and Graph are processed by a shared Transformer to get an unified representation, which is supervised by both fragment-level and molecular-level pre-training tasks.

DeepChem (Ramsundar et al., 2019) to parse it into a series of tokens  $S = [t_1, t_2, \dots, t_n]$ , then we apply an embedding layer to obtain the embeddings of SMILES denoted as  $\mathbf{s} = [s_1, s_2, \dots, s_n]$ , where  $s_i$  is the embedding of token  $i$  with size  $D$ . While an input graph is denoted as  $G = \{V, E\}$ , where  $V$  is the vertex set with  $v_i \in V$  denotes the  $i$ -th atom, and  $E$  is the edge set with  $e_{ij} \in E$  denotes an edge between the  $i$ -th and the  $j$ -th atom. We adopt a GCN (Li et al., 2020a) to obtain the graph embeddings  $\mathbf{g} = [g_1, g_2, \dots, g_m]$ , where  $m = |V|$  is the atom number, and  $g_i$  is the  $D$  dimensional vector for the  $i$ -th atom.

### 3.2 TRANSFORMER ENCODER

We adopt a Transformer based encoder denoted as  $\theta$  to handle both SMILES and graph embeddings. The typical Transformer takes a sequence of embeddings as input. We add a learnable position embeddings denoted as  $p_s$  to embeddings of SMILES  $\mathbf{s}$  to maintain positional information. As for the molecular graph in which atoms are not organized in sequence, we simply concatenate graph embeddings  $\mathbf{g}$  after the SMILES tokens embeddings to obtain the input of the Transformer, denoted as  $\mathbf{z}$ .

$$\mathbf{z} = [\mathbf{s} + p_s, \mathbf{g}].$$

The Transformer encoder is composed by stack of identical blocks, where each block consists of two parts: a multi-head self-attention (MSA) module and a feed-forward neural network (FFN). Specifically, the self-attention mechanism in MSA allows the cross-modality attention and conducts multi-modality interaction, including both inter- and intra-modality fusions.

To this end, the embeddings  $\mathbf{x} = \theta(\mathbf{z})$  is obtained for each molecule, where  $\mathbf{x} = (x_1, x_2, \dots, x_n, x_{n+1}, \dots, x_{n+m})$ ,  $x_i \in \mathbb{R}^D$ , in which the first  $n$  elements and the last  $m$  elements of  $\mathbf{x}$  stand for the corresponding SMILES and graph representations.

Afterward, we apply a typical average pooling operation (Huang et al., 2021) on  $\mathbf{x}$  to get the final molecular representation, denoted as  $x_{cls}$ .

$$x_{cls} = \frac{1}{m+n} \sum_{i=1}^{m+n} x_i.$$

Based on  $x_{cls}$ , different losses could be designed to facilitate the pre-training process. Considering the characteristics of SMILES and graph relation, we design both local (i.e. fragment-level) and global (i.e. molecular-level) losses.

### 3.3 SMILES-GRAPH FRAGMENT DECOMPOSITION

Our SMILES-graph fragment decomposition algorithm firstly apply mature method to decompose graph to different fragments, then assign each SMILES character to corresponding fragment, based on SMILES definition.

Specifically, we use BRICS (Degen et al., 2008) algorithm to split the molecular graph into different fragments, i.e.  $K_j$  fragments obtained for the  $j$ -th molecule, denoted as  $K$  for convenience. The labels of graph nodes could be represented as an vector  $\mathbf{l}_g = [l_1^{(g)}, l_2^{(g)}, \dots, l_m^{(g)}]$  to demonstrate which fragment each atom belongs to, where  $l_i^{(g)}$  stands for the fragment ID of the  $i$ -th atom with value from 0 to  $K - 1$ .

Since SMILES contains not only atoms but also special symbols representing chemical meanings, we define 4 rules as follows to label the special symbols, based on their meanings in SMILES grammar (Weininger, 1988). Each character of  $\{., -, =, \#, \$, :, /, \backslash\}$  is assigned the same label with its left nearest atom, because they denote the type of the corresponding bond started from the left nearest atom. The number after the character ‘C’ is assigned the same label with the character ‘C’, because the number usually indicates the beginning or the ending of a ring structure. The special sub-string ‘@@’ and ‘@’ are assigned the same fragment label with the carbon they decorate. Parentheses and brackets are assigned the same label with the nearest surrounding atom, because the content inside them are usually in a same fragment. After label assignment, the labels of SMILES tokens are denoted as  $\mathbf{l}_s = [l_1^{(s)}, l_2^{(s)}, \dots, l_n^{(s)}]$ , where  $l_i^{(s)}$  stands for the fragment ID of the  $i$ -th token with value from 0 to  $K - 1$ .

### 3.4 MULTI-LEVEL CROSS-MODALITY MASKING

We design two kinds of cross-modality mask language modeling methods in this paper, i.e. token-level masking and fragment-level cross-modality masking. For fragment-level masking, the goal is similar to previous conditional masking strategy (Chen et al., 2020b), i.e using the surrounding contexts and the full information from the other modality to recover the corresponding masked SMILES or graph fragments. However for tokens, we construct negative pairs and define the goal as only using surrounding context of single modality itself to predict the masked SMILES tokens or graph atoms, to emphasize the intra-modality pattern. In this way, both inter- and intra-modality patterns could be considered. This is reasonable because tokens are relatively smaller than fragments, and its context information in the same modality could be sufficient for MLM. Comparison with these masking strategies is conducted in ablation study.

Firstly, we introduce the token-level masking. For a given SMILES-graph pair  $(S, G)$ , we construct a negative pair  $(S, G')$  by randomly replacing the graph  $G$  to another molecular graph  $G'$  in the training set. After that, the input tokens of SMILES and atoms of graph are masked independently with the same ratio  $r_t$ . Specifically, for the SMILES, we randomly select  $|S| * r_t$  tokens from SMILES  $S$  to mask and predict the type of masked tokens. As for the graph, we randomly select  $|V| * r_t$  atoms, set the initial feature of both selected atoms and their adjacent edges to the pre-defined masked ones, then utilize GNN on the masked graph to obtain node embeddings. We follow the practice in GROVER to predict the masked atom’s contextual information, and the total loss is defined as follows.

$$L_t = - \sum_{\forall (S, G')} (\log P_{\theta}(\mathbf{s}_m | S_{\setminus m}, G'_{\setminus m}) + \log P_{\theta}(\mathbf{g}_m | S_{\setminus m}, G'_{\setminus m})).$$

where  $\mathbf{s}_m$  and  $\mathbf{g}_m$  stand for masked SMILES tokens, atoms and edges, respectively.  $S_{\setminus m}$  and  $G'_{\setminus m}$  stand for the surrounding contexts in the SMILES  $S$  and graph  $G'$ .

For fragment-level cross-modality masking (f-CMM), we randomly select  $r_f * K$  fragments and then randomly choose one modality with probability 0.5 to mask the selected fragments. The data

processing and predicting target are the same with token-level masking except taking fragments as masking unit. Thus the loss of f-CMM can be written as:

$$L_f = - \sum_{\forall(S,G)} (\log P_{\theta}(\mathbf{s}_m|S \setminus m, G) + \log P_{\theta}(\mathbf{g}_m|S, G \setminus m)),$$

where  $\mathbf{s}_m$  and  $\mathbf{g}_m$  stand for masked SMILES and graph fragments, respectively.  $S \setminus m$  and  $G \setminus m$  stand for the surrounding contexts in the SMILES  $S$  and graph  $G$ .

### 3.5 FRAGMENT-LEVEL ALIGNMENT

Fragment-level alignment (FLA) is a fine-grained cross-modality alignment strategy. The basic idea is to obtain corresponding fragment representations in a SMILES and graph pair, and then align them by a contrastive loss.

For each fragment  $i = 0, \dots, K - 1$ , the SMILES representation  $f_i^{(s)}$  is obtained by a multi-head attention layer with average pooling to aggregate the associated token embeddings, and the graph representation  $f_i^{(g)}$  is directly obtained by aggregating the associated atom embeddings with average pooling. Clearly,  $f_i^{(s)}$  and  $f_i^{(g)}$  form a positive pair because they stand for the same fragment in different modalities. While the negative pairs are constructed as follows. For each fragment  $f_i^{(s)}$ , the negative graph fragment set  $N_s$  includes both other fragments from the same graph and all fragments from other graphs. Similarly, we can obtain the negative SMILES fragment set  $N_g$  for each fragment  $f_i^{(g)}$ .

Afterward, we define the fragment-level contrastive learning loss as a combination of SMILES specific and graph specific contrastive losses, i.e.  $L_{FLA} = L_s + L_g$ , with

$$L_s = \frac{e^{\cos(f_i^{(s)}, f_i^{(g)})/\tau}}{e^{\cos(f_i^{(s)}, f_i^{(g)})/\tau} + \sum_{j \in N_s} e^{\cos(f_i^{(s)}, f_j^{(g)})/\tau}},$$

$$L_g = \frac{e^{\cos(f_i^{(g)}, f_i^{(s)})/\tau}}{e^{\cos(f_i^{(g)}, f_i^{(s)})/\tau} + \sum_{j \in N_g} e^{\cos(f_i^{(g)}, f_j^{(s)})/\tau}},$$

where  $\cos(\cdot)$  represents the cosine similarity function and  $\tau$  is the temperature hyper-parameter.

### 3.6 SMILES-GRAPH MATCHING

SMILES-Graph Matching is designed to reflect the molecular-level cross-modality alignment. Specifically, for each positive SMILES-graph pair  $(S, G)$ , we construct a negative pair  $(S, G')$  by randomly replacing the graph  $G$  to another molecular graph  $G'$  in the training set, and the corresponding molecular representations  $x_{cls}$  and  $x'_{cls}$  are then taken as input to a MLP head  $\theta_{sg}$  to predict the corresponding binary label 1 and 0, with loss as follows.

$$L_{SGM} = - \left( \sum_{\forall(S,G)} \log P_{\theta_{sg}}(x_{cls}) + \sum_{\forall(S,G')} \log(1 - P_{\theta_{sg}}(x'_{cls})) \right).$$

### 3.7 DOMAIN KNOWLEDGE LEARNING

We also design two pre-training losses to learn important chemical domain knowledge. Specifically, a MLP layer is added to predict the extended-connectivity fingerprints (Rogers & Hahn, 2010), which contains information about molecular topological structure and activity. The Mean Squared Error (MSE) loss is utilized for optimization. Furthermore, we add a classification layer to predict functional groups in a molecule, as in GROVER.

Table 1: Results in terms of mean and std for the 8 classification tasks from MoleculeNet benchmark, we report ROC-AUC(%) performance. The best and second best results are marked **bold** and underlined, respectively. ‘-’ denotes the case that the original results are not provided.

Method	BBBP	Sider	ClinTox	Bace	Tox21	Toxcast	HIV	MUV	Average
ChemBERTa	64.3(-)	-	73.3(-)	-	72.8(-)	-	62.2(-)	-	68.1
SMILES Transformer	70.4(-)	-	-	70.1(-)	-	-	72.9(-)	-	71.1
KCL	69.9(0.6)	63.6(0.8)	58.8(1.9)	80.2(1.8)	70.6(0.5)	63.8(0.1)	75.7(0.6)	70.4(0.9)	69.1
GROVER(base)	71.9(0.1)	65.6(0.9)	81.7(2.5)	83.3(0.1)	73.6(0.3)	66.1(0.1)	75.0(0.2)	76.7(0.2)	74.2
GROVER(large)	71.8(0.5)	<b>66.8(0.1)</b>	73.9(5.6)	83.5(0.1)	73.4(0.1)	65.9(0.2)	73.1(1.7)	72.1(5.5)	72.6
AttrMasking	64.3(2.8)	61.0(0.7)	71.8(4.1)	79.3(1.6)	76.7(0.4)	64.2(0.5)	77.2(1.1)	74.7(1.4)	71.2
ContextPred	68.0(2.0)	60.9(0.6)	65.9(3.8)	79.6(1.2)	75.7(0.7)	63.9(0.6)	77.3(1.0)	75.8(1.7)	70.9
GraphLoG	72.5(0.8)	61.2(1.1)	76.7(3.3)	83.5(1.2)	75.7(0.5)	63.5(0.7)	77.8(0.8)	76.0(1.1)	73.4
GraphMAE	72.0(0.6)	60.3(1.1)	82.3(1.2)	83.1(0.9)	75.5(0.6)	64.1(0.3)	77.2(1.0)	76.3(2.4)	73.8
MGSSL	70.5(1.1)	60.5(0.7)	79.7(2.2)	79.7(0.8)	76.4(0.4)	63.8(0.3)	79.5(1.1)	78.1(1.8)	73.5
Mole-BERT	72.3(0.7)	62.2(0.8)	80.1(3.6)	81.4(1.0)	77.1(0.4)	64.5(0.4)	78.6(0.7)	78.3(1.2)	74.3
GraphMVP	72.4(1.6)	63.9(1.2)	79.1(2.8)	81.2(0.9)	75.9(0.5)	63.1(0.4)	77.0(1.2)	77.7(0.6)	73.8
3D InfoMax	69.10(1.07)	53.37(3.34)	59.43(3.21)	79.42(1.94)	74.46(0.74)	64.41(0.88)	-	76.08(1.33)	68.0
MOCO	71.6(1.0)	61.2(0.6)	81.6(3.7)	82.6(0.3)	76.7(0.4)	64.9(0.8)	78.3(0.4)	78.5(1.4)	74.4
UniMAP	<b>75.6(1.8)</b>	66.6(0.8)	<b>98.3(1.7)</b>	<b>83.6(1.0)</b>	<b>77.2(0.9)</b>	<b>67.0(0.4)</b>	<b>80.1(0.7)</b>	<b>78.9(1.4)</b>	<b>78.4</b>

## 4 EXPERIMENTS

This section introduces our experimental evaluation of UniMAP on three different kinds of downstream tasks, including molecular property prediction, drug-target affinity prediction, and drug-drug interaction prediction.

For pre-training, we select about 10 millions molecules from PubChem, which is a widely used and publicly accessible database in chemistry, it contains about 114 millions compounds which mostly are small molecules. In the data preprocessing phase, SMILES are canonicalized and converted to molecular graph by RDKit (Landrum et al., 2013). In the training phase, we adopt the RoBERTa model as the multi-modality encoder  $\theta$  and utilize Adam for optimization. Specifically, we utilize the Roberta base model as the shared transformer which contains 12 layers and the hidden size of embedding is set to 768. For optimization, the initial learning rate is set to 0.00005, and is then decreased by a linear decay scheduler. The mask ratio of token-level masking and fragment-level cross-modality masking are set as 0.2 and 0.6 separately, and the temperature  $\tau$  of contrastive learning in fragment-level alignment is set as 0.05. Since we have multiple pre-training losses, the model is trained in a multi-task learning manner, and the weight of each per-training task is equal to 1. We train our model for 40 epochs on a 8xV100 GPUs machine. The batch size per GPU is set to 64. In total, it takes about 10 days to finish the training process, and half precision training is utilized to save GPU memory.

### 4.1 MOLECULAR PROPERTY PREDICTION

**Data.** We experiment on MoleculeNet (Wu et al., 2018), a widely used benchmark, to test the molecular property prediction ability, including three biophysics properties(i.e. Bace, HIV, and MUV) and five physiology properties (i.e. BBBP, Sider, ClinTox, Tox21, and Toxcast). Following previous practices in MoleculeNet, each dataset is split to train, validation and test set with ratio 8:1:1, based on the scaffold splitter of DeepChem. Since the targets are classification tasks, we use ROC-AUC(%) as the evaluation metric. Specially for UniMAP, we run 3 times with different random seed for each dataset, and report the mean and standard deviation value.

**Baseline Methods.** We compare UniMAP with various pre-training baselines, including SMILES based methods ChemBERTa (Chithrananda et al., 2020) and SMILES Transformer (Honda et al., 2019), graph based methods KCL (Fang et al., 2022b), GROVER (Rong et al., 2020), AttrMasking (Hu et al., 2019), ContextPred (Hu et al., 2019), GraphLoG (Xu et al., 2021), GraphMAE (Hou et al., 2022), MGSSL (Zhang et al., 2021), and Mole-BERT (Anonymous, 2023), 3D based methods 3D InfoMax (Stärk et al., 2022) and GraphMVP (Liu et al., 2022), and hybrid method MOCO (Zhu et al., 2022). Most results are from the original paper except KCL and GROVER, since they use different data split methods. To guarantee a fair comparison, we employ their pre-trained models and conduct fine-tuning on the same data with other baselines for evaluation.

**Fine-Tuning UniMAP.** Based on the pre-trained representation  $x_{cls}$ , a two-layer MLP is adopted to obtain the final classification label, supervised by a corresponding classification loss, i.e. cross

Table 2: Results in terms of mean and std for the 4 regression tasks. We report RMSE scores, the best and second best results are marked as **bold** and underlined, respectively.

Method	ESOL	Lipo	Malaria	CEP
GROVER(base)	0.904(0.061)	0.815(0.012)	1.092(0.007)	1.339(0.005)
GROVER(large)	0.951(0.027)	0.803(0.038)	1.082(0.009)	1.353(0.004)
GraphMVP	1.064(0.045)	0.691(0.013)	1.106(0.013)	1.228(0.001)
Mole-BERT	1.015(0.030)	0.676(0.017)	1.074(0.009)	1.232(0.009)
MOCO	0.984(0.034)	0.707(0.001)	1.093(0.009)	<b>1.101(0.007)</b>
UniMAP	<b>0.861(0.010)</b>	<b>0.664(0.023)</b>	<b>1.043(0.007)</b>	1.128(0.007)

entropy. For each task, we try 20 different hyper-parameter combinations, including learning rate, batch size and weight-decay, via grid search on the validation set and report the best results.

**Results.** As shown in Table 1, UniMAP achieves the best results on 7 out of 8 datasets, while on Sider our result of 66.6% is the second best, which is slightly worse than GROVER’s 66.8%. Specifically from the averaged results, we can see that UniMAP (i.e. 78.4%) significantly outperform the second best method MOCO (i.e. 74.4%), which is also a hybrid method that combines four different molecular data forms. These results confirm the strength of UniMAP to perform consistently better on various molecular property prediction datasets from MoleculeNet, by using both SMILES and graph representation with fine-grained alignment.

Beyond the classification tasks, we also verify our method’s effectiveness on 4 regression tasks: ESOL (Delaney, 2004) contains regression labels measuring the molecular water solubility. Lipophilicity(Lipo), which is a subset of ChEMBL (Gaulton et al., 2012), consists of experimental results of octanol/water distribution coefficient. CEP records the organic photovoltaic efficiency of molecules selected from the Havard Clean Energy Project(CEP) (Hachmann et al., 2011). Malaria (Gamo et al., 2010) takes drug efficacy against malaria, which is a type of disease caused by parasites, as regression target. We choose the top 4 methods based on the averaged classification results in Table 1 for comparison. That is to say, MOCO, Mole-BERT, GROVER and GraphMVP are treated as our baseline methods. Similarly, a two-layer MLP is adopted to obtain the final regression value of UniMAP, supervised by a corresponding regression loss, i.e. MAE. RMSE is utilized as the evaluation metric. From the results in Table 2, we can see that UniMAP performs the best on three tasks, and second best on the other one.

## 4.2 DRUG-TARGET AFFINITY PREDICTION

**Data.** Drug-Target Affinity (DTA) prediction is an important task in drug discovery, which is designed to predict the binding affinity between a drug and target protein. We evaluate our method on two widely used DTA benchmarks, DAVIS (Davis et al., 2011) and KIBA (Tang et al., 2014). DAVIS records dissociation constant( $K_d$ ) value of kinase protein and its inhibitors, while KIBA contains the  $K_i$ ,  $K_d$  and  $IC_{50}$  values to describe the bioactivity of kinase inhibitors. We follow GraphMVP to split the datasets and calculate the MSE and Concordance Index (CI) scores as evaluate metrics.

**Baseline Models.** We compare our method with three different types of baselines. KronRLS (Panico et al., 1993), GraphDTA (Nguyen et al., 2021) and DeepDTA (Öztürk et al., 2018) are supervised methods for DTA; SMT-DTA (Pei et al., 2022) is a semi-supervised method, which trains the model with an additional unsupervised masked language modeling task with large-scale unlabeled molecules and protein data; GraphMVP and Mole-BERT are molecular pre-training methods.

**Fine-Tuning UniMAP.** Similarly to GraphMVP, we model the target protein with a convolution neural network to get the protein embedding, concatenate it with the molecular embedding  $x_{cls}$ , and then use an MLP to obtain the predicted binding affinity value.

**Results.** The results are demonstrated in Table 3. We report MSE and Concordance Index(CI) scores as evaluation metrics, GraphMVP and Mole-BERT didn’t provide CI scores in their original results. From the results, we can see that UniMAP outperforms all supervised DTA methods and other molecular pre-training methods, and performs slightly worse then SMT-DTA. It may because SMT-DTA utilized large-scale unlabeled protein data and a more complicated Transformer to learn

Table 3: Experiment results on DTA benchmarks. We report MSE and Concordance Index (CI) scores, the best and second best results are marked **bold** and underlined, respectively.

Task Method	Davis		KIBA	
	MSE↓	CI↑	MSE↓	CI↑
KronRLS	0.329	0.847	0.852	0.688
GraphDTA	0.263	0.864	0.183	0.862
DeepDTA	0.262	0.870	0.196	0.864
SMT-DTA	<b>0.219</b>	<b>0.890</b>	<u>0.154</u>	<b>0.894</b>
GraphMVP	0.274	-	0.175	-
Mole-BERT	0.266	-	0.157	-
<b>UniMAP</b>	<u>0.246</u>	<u>0.888</u>	<b>0.144</b>	<u>0.891</u>

Table 4: Results for DDI task. We report the accuracy, precision, recall and F1-score, the best and second best results are marked **bold** and underlined, respectively.

Method	Accuracy	Precision	Recall	F1-score
DeepDDI	0.877	0.799	0.759	0.766
DeepWalk	0.800	0.822	0.710	0.747
LINE	0.751	0.687	0.545	0.580
MUFFIN	0.939	0.926	0.908	0.911
MUFFIN_KG	<u>0.965</u>	<u>0.957</u>	<b>0.948</b>	<u>0.950</u>
X-MOL	0.952	-	-	-
PanGu	0.957	-	-	-
<b>UniMAP</b>	<b>0.972</b>	<b>0.958</b>	<u>0.943</u>	<b>0.952</b>

the protein embedding. Still, UniMAP performs better in terms of MSE in KIBA, indicating the ability of UniMAP to learn a meaningful representation for DTA.

### 4.3 DRUG-DRUG INTERACTION PREDICTION

**Data.** In addition to molecular property prediction and drug-target affinity prediction, we also conduct experiments on the drug-drug interaction (DDI) prediction task, which plays a crucial role in drug repositioning and virtual screening. Specifically, we experiment on the DrugBank Multi-Typed DDI dataset (Ryu et al., 2018), which contains 192,284 DDI pairs covering 86 interaction types. The objective is to predict the interaction type of each drug pair. The dataset is split to train, validation and test set with the ratio 3:1:1. We randomly split the data for 3 times with different seeds and report the mean value of evaluation metrics, including accuracy, precision, recall and F1-score as in Chen et al. (2021).

**Baseline Models.** We compare UniMAP with different kinds of baselines, including deep learning method DeepDDI (Ryu et al., 2018), graph embedding methods DeepWalk (Perozzi et al., 2014) and LINE (Tang et al., 2015), and some recent pre-training methods such as MUFFIN (Chen et al., 2021), MUFFIN\_KG (Chen et al., 2021), X-MOL (Xue et al., 2021) and PanGu (Lin et al., 2022). Please note that we use MUFFIN\_KG to refer to the MUFFIN variant with an extra knowledge graph branch.

**Fine-Tuning UniMAP.** For the downstream fine-tuning of UniMAP, we first concatenate the representation  $x_{cls}$  of the two paired drugs as the input, and then feed it to a two-layer MLP for multi-class prediction.

**Results.** The experimental results are shown in Table 4. Here we report four metrics including accuracy, precision, recall and F1-score, where X-MOL and PanGu only show the accuracy result in their original paper. We can see that all pre-training methods (MUFFIN, MUFFIN\_KG, X-MOL, Pangu, and UniMAP) outperform deep learning method (DeepDDI) and graph embedding methods (DeepWalk and LINE), demonstrating the benefit of pre-training. More importantly, UniMAP consistently outperforms the pre-training methods in terms of all the four metrics, except for the recall compared with MUFFIN\_KG. This may be because MUFFIN\_KG utilizes extra knowledge graph information, which is not considered in both UniMAP and other pre-training baselines. Therefore,

UniMAP shows better DDI prediction results by leveraging multi-modality pre-training, compared with single-modality pre-training methods, such as MUFFIN, X-MOL, and PanGu.

## 5 DISCUSSIONS

In this section, we provide an ablation study of losses and visualization results, to facilitate further understanding of UniMAP.

Table 5: Comparison with different loss combinations.

Method	BBBP	Sider	ClinTox	Bace	Tox21	Toxcast	HIV	MUV	Average
SGM + CMM + FLA + DKL	<b>76.1(0.4)</b>	<b>65.8(0.1)</b>	98.6(0.2)	80.9(0.3)	<b>76.3(0.6)</b>	60.1(0.4)	77.1(0.4)	72.6(0.3)	<b>75.9</b>
SGM + CMM + FLA	75.0(0.4)	63.6(0.4)	<b>98.7(0.2)</b>	<b>81.2(0.8)</b>	74.9(0.3)	<b>60.8(0.8)</b>	<b>77.6(1.5)</b>	71.8(1.4)	<u>75.5</u>
SGM + CMM	<u>71.1(0.1)</u>	63.8(0.3)	98.1(0.4)	80.1(0.8)	75.4(0.2)	59.4(0.6)	76.5(0.9)	<b>72.8(1.1)</b>	74.6
SGM + Conditional Masking	71.1(0.5)	<u>60.7(0.6)</u>	96.4(0.8)	79.3(0.3)	74.6(0.1)	58.1(1.8)	72.2(0.3)	67.7(0.7)	72.5
SGM + Single-Modality Masking	71.0(0.3)	61.7(0.4)	95.8(0.7)	79.2(1.4)	75.6(0.2)	57.4(0.4)	75.7(0.1)	69.3(0.7)	73.2

### 5.1 ABLATION STUDY ON DIFFERENT LOSSES

Our ablation study contains two parts, comparing different losses, and different masking strategies. We test on 8 typical classification tasks, and the results are shown in Table 5.

Firstly, we delete DKL and FLA one by one. From the results, we can see that DKL is helpful for BBBP, Sider, Tox21, and MUV, while FLA is useful for BBBP, ClinTox, Bace, Toxcast and HIV. Though it is difficult to explain why one loss is especially useful for one specific task, these results show a clear complementary effect of global molecular-level pre-training loss (DKL) and fine-grained local semantic representation loss (FLA).

Along with the SGM task which is commonly adopted in existing multi-modal methods, we compare CMM in UniMAP with the other two token-level mask strategies, i.e. token-level conditional masking and single-modality masking. Specifically, token-level conditional masking means that we only mask one-modality tokens, i.e. SMILES tokens or graph atoms, to conduct the prediction based on two modality data; while single-modality masking means that the model predicts the masked tokens from only the surrounding tokens of the same modality. The results show that our CMM performs the best on most tasks, except on Tox21 (i.e. slightly worse than conditional masking). Therefore, we can see that an in-depth multi-modality dependency strategy will produce a better molecular representation.

### 5.2 EMBEDDING CLUSTERING RESULTS

We conduct visualization analyses on the output embeddings from both molecular and fragment level.

Firstly, we randomly select about two thousands molecules belonging to pre-defined 16 types of scaffold (denoted as different colors), then visualize their UniMAP representations through t-SNE (Van der Maaten & Hinton, 2008). The results are shown in Figure 3. We can see that the learned representations demonstrate a clear scaffold clustering property, i.e. molecules with the same scaffold are mapped to close positions in the embedding space.

In addition, we visualize the embeddings of four thousands molecular fragments, as shown in Figure 4. We find that some clustered fragments correspond to certain chemical categories (Clayden et al., 2012). For example, four adjacent clusters colored in light yellow, light grey, bright green and magenta stand for Fluoride, Chloride, Bromide and Iodide respectively, which contain different atom of halogens like F, Cl, Br and I. Three clusters colored in red, blue and magenta imply Alkane, Thioalkane, and Bromoalkane respectively. We also find three nitrogenous fragment clusters including Nitrile, Amide and Nitro compound, and two heterocycle clusters including Oxygen heterocycle and Oxidized nitrogen heterocycle.

From the above visualization results, we can conclude that UniMAP provides meaningful molecular-level and fragment-level representations.

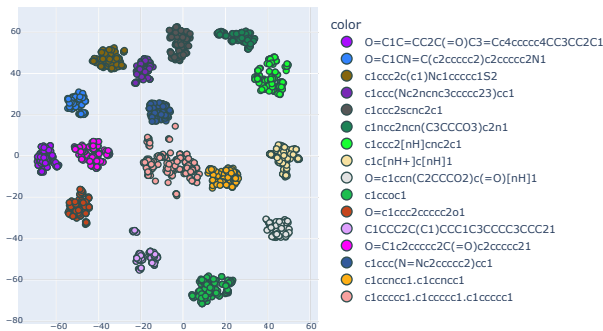


Figure 3: Visualization of molecular embeddings with colors indicating different scaffolds.

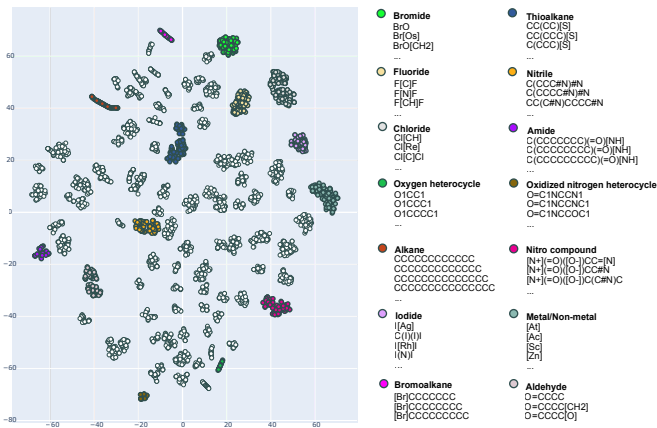


Figure 4: Visualization of fragment embeddings. Several clusters are labeled with colors indicating different categories, of which chemical name following several representative fragments are listed on the right.

### 5.3 FRAGMENT ALIGNMENT PATTERN

Inspired by the analysis in NLP (Clark et al., 2019) that higher layer attention weights usually demonstrate some learned patterns, we visualize the learned attention weights at the 8-th layer. Interestingly, we find that the learned model demonstrates a clear fragment alignment pattern. We give three example molecules as case study, as shown in Figure 5. Given the SMILES and graph representation of a molecule, multiple fragments are obtained, labeled with different colors, and the attention weights between different SMILES tokens and graph atoms are presented to lines with different color depth, where deeper color means higher attention weight. Clearly, the larger attention weights are obtained between SMILES tokens and graph atoms within the same corresponding fragment, validating the soundness of UniMAP.

## 6 CONCLUSION

In this paper, we propose the first single-stream multi-modality model for molecular representation learning, namely UniMAP. Firstly, a SMILES-graph decomposition algorithm is designed to obtain corresponding SMILES and graph fragments, which together with tokens function as heterogeneous input in pre-training tasks. Secondly, a shared Transformer is utilized to conduct deep cross-modality fusion. Besides molecular-level tasks such as SMILES-Graph Matching and Domain Knowledge Learning, we introduce two novel fragment-level pre-training tasks, i.e. Multi-Level Cross-Modality Masking and Fragment-Level Alignment. Finally, we conduct extensive experiments on three different kinds of downstream tasks, including molecular property prediction, drug-target affinity prediction and drug-drug interaction. Our experimental results show that UniMAP significantly outperforms existing supervised and pre-training methods. We also conduct an ablation

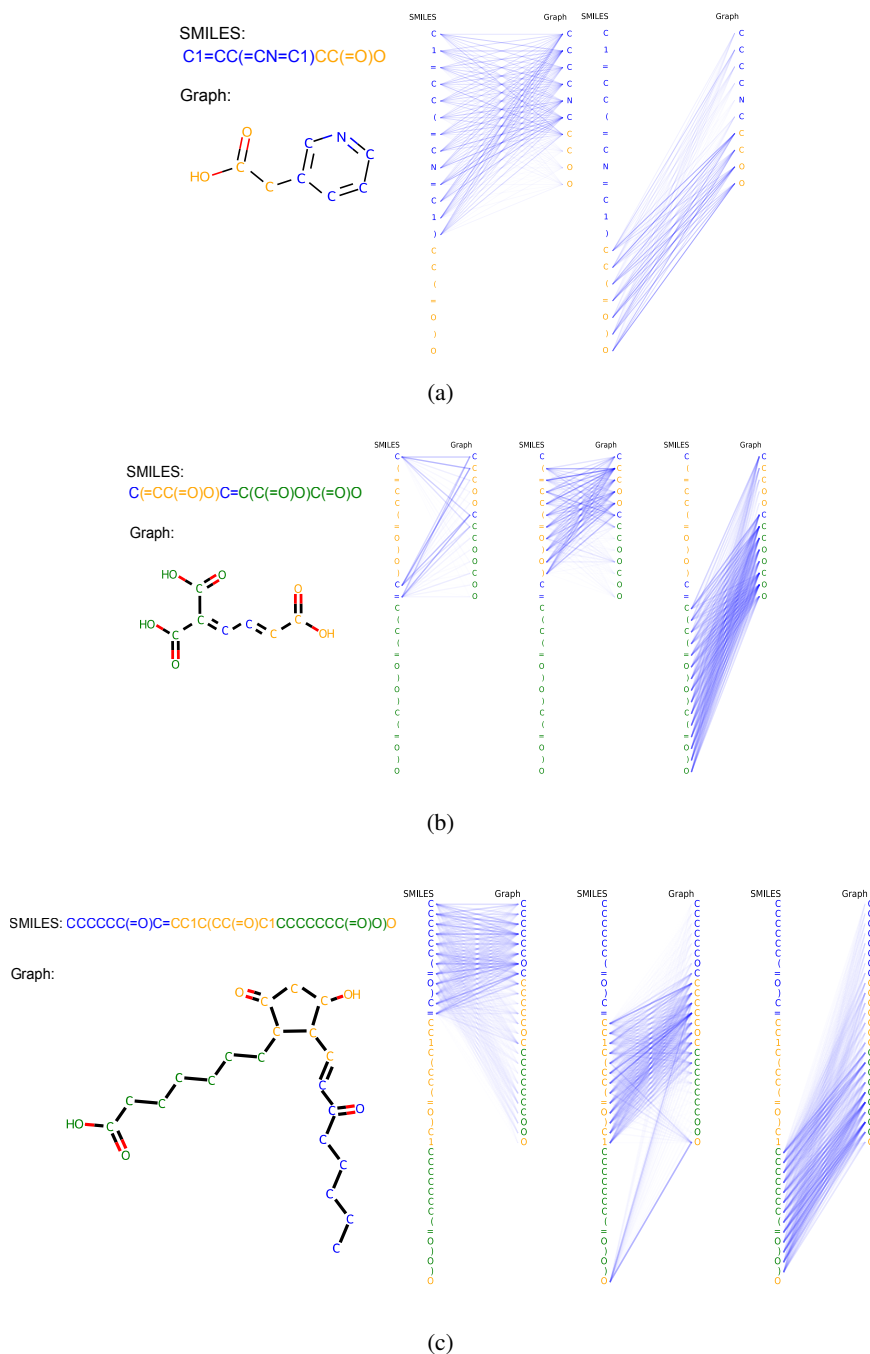


Figure 5: Visualization of attentions from SMILES to graph.

study on the effect of different losses, and observe an interesting complementary relation between global molecular-level pre-training loss and fine-grained local semantic representation loss. Furthermore, we conduct a visualization analysis on the output embeddings, and find that the clusters of both molecular and fragment representations demonstrate meaningful chemical properties. In addition, the learned attention weights of UniMAP show a clear fragment alignment pattern, validating the soundness of UniMAP.

Though this paper focuses on SMILES and graph data fusion, our proposed UniMAP is a modality-agnostic framework and therefore has the potential to be extended to a universal model, including

various molecular data formats and downstream tasks, which could inspire diverse directions for future exploration.

## REFERENCES

- Anonymous. Mole-BERT: Rethinking pre-training graph neural networks for molecules. In *Submitted to The Eleventh International Conference on Learning Representations*, 2023. URL <https://openreview.net/forum?id=jevY-DtiZTR>. under review.
- Deli Chen, Yankai Lin, Wei Li, Peng Li, Jie Zhou, and Xu Sun. Measuring and relieving the over-smoothing problem for graph neural networks from the topological view. In *Proceedings of the AAAI Conference on Artificial Intelligence*, volume 34, pp. 3438–3445, 2020a.
- Yen-Chun Chen, Linjie Li, Licheng Yu, Ahmed El Kholy, Faisal Ahmed, Zhe Gan, Yu Cheng, and Jingjing Liu. Uniter: Universal image-text representation learning. In *European conference on computer vision*, pp. 104–120. Springer, 2020b.
- Yujie Chen, Tengfei Ma, Xixi Yang, Jianmin Wang, Bosheng Song, and Xiangxiang Zeng. Muffin: multi-scale feature fusion for drug–drug interaction prediction. *Bioinformatics*, 37(17):2651–2658, 2021.
- Seyone Chithrananda, Gabriel Grand, and Bharath Ramsundar. Chemberta: large-scale self-supervised pretraining for molecular property prediction. *arXiv preprint arXiv:2010.09885*, 2020.
- Kevin Clark, Urvashi Khandelwal, Omer Levy, and Christopher D Manning. What does bert look at? an analysis of bert’s attention. *arXiv preprint arXiv:1906.04341*, 2019.
- Jonathan Clayden, Nick Greeves, and Stuart Warren. *Organic chemistry*. Oxford university press, 2012.
- Mindy I Davis, Jeremy P Hunt, Sanna Herrgard, Pietro Ciceri, Lisa M Wodicka, Gabriel Pallares, Michael Hocker, Daniel K Treiber, and Patrick P Zarrinkar. Comprehensive analysis of kinase inhibitor selectivity. *Nature biotechnology*, 29(11):1046–1051, 2011.
- Jörg Degen, Christof Wegscheid-Gerlach, Andrea Zaliani, and Matthias Rarey. On the art of compiling and using ‘drug-like’ chemical fragment spaces. *ChemMedChem: Chemistry Enabling Drug Discovery*, 3(10):1503–1507, 2008.
- John S Delaney. Esol: estimating aqueous solubility directly from molecular structure. *Journal of chemical information and computer sciences*, 44(3):1000–1005, 2004.
- Jacob Devlin, Ming-Wei Chang, Kenton Lee, and Kristina Toutanova. BERT: Pre-training of deep bidirectional transformers for language understanding. In *Proceedings of the 2019 Conference of the North American Chapter of the Association for Computational Linguistics: Human Language Technologies, Volume 1 (Long and Short Papers)*, pp. 4171–4186, Minneapolis, Minnesota, June 2019. Association for Computational Linguistics. doi: 10.18653/v1/N19-1423. URL <https://aclanthology.org/N19-1423>.
- Xiaomin Fang, Lihang Liu, Jieqiong Lei, Donglong He, Shanzhuo Zhang, Jingbo Zhou, Fan Wang, Hua Wu, and Haifeng Wang. Geometry-enhanced molecular representation learning for property prediction. *Nature Machine Intelligence*, 4(2):127–134, 2022a.
- Yin Fang, Qiang Zhang, Haihong Yang, Xiang Zhuang, Shumin Deng, Wen Zhang, Ming Qin, Zhuo Chen, Xiaohui Fan, and Huajun Chen. Molecular contrastive learning with chemical element knowledge graph. In *Proceedings of the AAAI Conference on Artificial Intelligence*, volume 36, pp. 3968–3976, 2022b.
- Francisco-Javier Gamo, Laura M Sanz, Jaume Vidal, Cristina De Cozar, Emilio Alvarez, Jose-Luis Lavandera, Dana E Vanderwall, Darren VS Green, Vinod Kumar, Samiul Hasan, et al. Thousands of chemical starting points for antimalarial lead identification. *Nature*, 465(7296):305–310, 2010.
- Anna Gaulton, Louisa J Bellis, A Patricia Bento, Jon Chambers, Mark Davies, Anne Hersey, Yvonne Light, Shaun McGlinchey, David Michalovich, Bissan Al-Lazikani, et al. ChEMBL: a large-scale bioactivity database for drug discovery. *Nucleic acids research*, 40(D1):D1100–D1107, 2012.

- Zhihui Guo, Pramod Sharma, Andy Martinez, Liang Du, and Robin Abraham. Multilingual molecular representation learning via contrastive pre-training. In *Proceedings of the 60th Annual Meeting of the Association for Computational Linguistics (Volume 1: Long Papers)*, pp. 3441–3453, 2022.
- Johannes Hachmann, Roberto Olivares-Amaya, Sule Atahan-Evrenk, Carlos Amador-Bedolla, Roel S Sánchez-Carrera, Aryeh Gold-Parker, Leslie Vogt, Anna M Brockway, and Alán Aspuru-Guzik. The harvard clean energy project: large-scale computational screening and design of organic photovoltaics on the world community grid. *The Journal of Physical Chemistry Letters*, 2(17):2241–2251, 2011.
- Shion Honda, Shoi Shi, and Hiroki R Ueda. Smiles transformer: Pre-trained molecular fingerprint for low data drug discovery. *arXiv preprint arXiv:1911.04738*, 2019.
- Zhenyu Hou, Xiao Liu, Yuxiao Dong, Chunjie Wang, Jie Tang, et al. Graphmae: Self-supervised masked graph autoencoders. *arXiv preprint arXiv:2205.10803*, 2022.
- Weihua Hu, Bowen Liu, Joseph Gomes, Marinka Zitnik, Percy Liang, Vijay Pande, and Jure Leskovec. Strategies for pre-training graph neural networks. In *International Conference on Learning Representations*, 2019.
- Junjie Huang, Duyu Tang, Wanjun Zhong, Shuai Lu, Linjun Shou, Ming Gong, Daxin Jiang, and Nan Duan. Whiteningbert: An easy unsupervised sentence embedding approach. *arXiv preprint arXiv:2104.01767*, 2021.
- Yuqi Huo, Manli Zhang, Guangzhen Liu, Haoyu Lu, Yizhao Gao, Guoxing Yang, Jingyuan Wen, Heng Zhang, Baogui Xu, Weihao Zheng, et al. Wenlan: Bridging vision and language by large-scale multi-modal pre-training. *arXiv preprint arXiv:2103.06561*, 2021.
- Chao Jia, Yinfei Yang, Ye Xia, Yi-Ting Chen, Zarana Parekh, Hieu Pham, Quoc Le, Yun-Hsuan Sung, Zhen Li, and Tom Duerig. Scaling up visual and vision-language representation learning with noisy text supervision. In *International Conference on Machine Learning*, pp. 4904–4916. PMLR, 2021.
- Rui Jiao, Jiaqi Han, Wenbing Huang, Yu Rong, and Yang Liu. Energy-motivated equivariant pre-training for 3d molecular graphs. *arXiv preprint arXiv:2207.08824*, 2022.
- Sunghwan Kim, Jie Chen, Tiejun Cheng, Asta Gindulyte, Jia He, Siqian He, Qingliang Li, Benjamin A Shoemaker, Paul A Thiessen, Bo Yu, et al. Pubchem 2019 update: improved access to chemical data. *Nucleic acids research*, 47(D1):D1102–D1109, 2019.
- Talia B Kimber, Yonghui Chen, and Andrea Volkamer. Deep learning in virtual screening: recent applications and developments. *International Journal of Molecular Sciences*, 22(9):4435, 2021.
- Mario Krenn, Florian Häse, AkshatKumar Nigam, Pascal Friederich, and Alan Aspuru-Guzik. Self-referencing embedded strings (selfies): A 100% robust molecular string representation. *Machine Learning: Science and Technology*, 1(4):045024, 2020.
- Greg Landrum et al. Rdkit: A software suite for cheminformatics, computational chemistry, and predictive modeling. *Greg Landrum*, 2013.
- Xiao Qing Lewell, Duncan B Judd, Stephen P Watson, and Michael M Hann. Recap retrosynthetic combinatorial analysis procedure: a powerful new technique for identifying privileged molecular fragments with useful applications in combinatorial chemistry. *Journal of chemical information and computer sciences*, 38(3):511–522, 1998.
- Chenliang Li, Ming Yan, Haiyang Xu, Fuli Luo, Wei Wang, Bin Bi, and Songfang Huang. Semvlp: Vision-language pre-training by aligning semantics at multiple levels. *arXiv preprint arXiv:2103.07829*, 2021a.
- Guohao Li, Chenxin Xiong, Ali Thabet, and Bernard Ghanem. Deepergcn: All you need to train deeper gcns. *arXiv preprint arXiv:2006.07739*, 2020a.

- Pengyong Li, Jun Wang, Yixuan Qiao, Hao Chen, Yihuan Yu, Xiaojun Yao, Peng Gao, Guotong Xie, and Sen Song. An effective self-supervised framework for learning expressive molecular global representations to drug discovery. *Briefings in Bioinformatics*, 22(6):bbab109, 2021b.
- Shuangli Li, Jingbo Zhou, Tong Xu, Dejing Dou, and Hui Xiong. Geomgcl: Geometric graph contrastive learning for molecular property prediction. In *Proceedings of the AAAI Conference on Artificial Intelligence*, volume 36, pp. 4541–4549, 2022.
- Xiujun Li, Xi Yin, Chunyuan Li, Pengchuan Zhang, Xiaowei Hu, Lei Zhang, Lijuan Wang, Houdong Hu, Li Dong, Furu Wei, et al. Oscar: Object-semantics aligned pre-training for vision-language tasks. In *European Conference on Computer Vision*, pp. 121–137. Springer, 2020b.
- Xinyuan Lin, Chi Xu, Zhaoping Xiong, Xinfeng Zhang, Ningxi Ni, Bolin Ni, Jianlong Chang, Ruiqing Pan, Zidong Wang, Fan Yu, et al. Pangu drug model: Learn a molecule like a human. *bioRxiv*, 2022.
- Shengchao Liu, Hanchen Wang, Weiyang Liu, Joan Lasenby, Hongyu Guo, and Jian Tang. Pre-training molecular graph representation with 3d geometry. In *International Conference on Learning Representations*, 2022. URL <https://openreview.net/forum?id=xQUe1pOKPam>.
- Tairan Liu, Misagh Naderi, Chris Alvin, Supratik Mukhopadhyay, and Michal Brylinski. Break down in order to build up: decomposing small molecules for fragment-based drug design with e molfrag. *Journal of chemical information and modeling*, 57(4):627–631, 2017.
- Yinhan Liu, Myle Ott, Naman Goyal, Jingfei Du, Mandar Joshi, Danqi Chen, Omer Levy, Mike Lewis, Luke Zettlemoyer, and Veselin Stoyanov. Roberta: A robustly optimized bert pretraining approach, 2019. URL <https://arxiv.org/abs/1907.11692>.
- Shengjie Luo, Tianlang Chen, Yixian Xu, Shuxin Zheng, Tie-Yan Liu, Liwei Wang, and Di He. One transformer can understand both 2d & 3d molecular data. *arXiv preprint arXiv:2210.01765*, 2022.
- Harry L Morgan. The generation of a unique machine description for chemical structures—a technique developed at chemical abstracts service. *Journal of chemical documentation*, 5(2):107–113, 1965.
- Thin Nguyen, Hang Le, Thomas P Quinn, Tri Nguyen, Thuc Duy Le, and Svetha Venkatesh. Graphdta: Predicting drug–target binding affinity with graph neural networks. *Bioinformatics*, 37(8):1140–1147, 2021.
- Hakime Öztürk, Arzucan Özgür, and Elif Ozkirimli. Deepdta: deep drug–target binding affinity prediction. *Bioinformatics*, 34(17):i821–i829, 2018.
- R Panico, WH Powell, and Jean-Claude Richer. *A guide to IUPAC Nomenclature of Organic Compounds*, volume 2. Blackwell Scientific Publications, Oxford, 1993.
- Qizhi Pei, Lijun Wu, Jinhua Zhu, Yingce Xia, Shufang Xia, Tao Qin, Haiguang Liu, and Tie-Yan Liu. Smt-dta: Improving drug-target affinity prediction with semi-supervised multi-task training. *arXiv preprint arXiv:2206.09818*, 2022.
- Bryan Perozzi, Rami Al-Rfou, and Steven Skiena. Deepwalk: Online learning of social representations. In *Proceedings of the 20th ACM SIGKDD international conference on Knowledge discovery and data mining*, pp. 701–710, 2014.
- Daniil Polykovskiy, Alexander Zhebrak, Benjamin Sanchez-Lengeling, Sergey Golovanov, Oktai Tatanov, Stanislav Belyaev, Rauf Kurbanov, Aleksey Artamonov, Vladimir Aladinskiy, Mark Veselov, et al. Molecular sets (moses): a benchmarking platform for molecular generation models. *Frontiers in pharmacology*, 11:565644, 2020.
- Alec Radford, Jong Wook Kim, Chris Hallacy, Aditya Ramesh, Gabriel Goh, Sandhini Agarwal, Girish Sastry, Amanda Askell, Pamela Mishkin, Jack Clark, et al. Learning transferable visual models from natural language supervision. In *International Conference on Machine Learning*, pp. 8748–8763. PMLR, 2021.

- Bharath Ramsundar, Peter Eastman, Patrick Walters, Vijay Pande, Karl Leswing, and Zhenqin Wu. *Deep Learning for the Life Sciences*. O’Reilly Media, 2019. <https://www.amazon.com/Deep-Learning-Life-Sciences-Microscopy/dp/1492039837>.
- David Rogers and Mathew Hahn. Extended-connectivity fingerprints. *Journal of chemical information and modeling*, 50(5):742–754, 2010.
- Yu Rong, Yatao Bian, Tingyang Xu, Weiyang Xie, Ying Wei, Wenbing Huang, and Junzhou Huang. Self-supervised graph transformer on large-scale molecular data. *Advances in Neural Information Processing Systems*, 33:12559–12571, 2020.
- Jae Yong Ryu, Hyun Uk Kim, and Sang Yup Lee. Deep learning improves prediction of drug–drug and drug–food interactions. *Proceedings of the National Academy of Sciences*, 115(18):E4304–E4311, 2018.
- Ana Sanchez-Fernandez, Elisabeth Rumetshofer, Sepp Hochreiter, and Günter Klambauer. Contrastive learning of image- and structure-based representations in drug discovery. In *ICLR2022 Machine Learning for Drug Discovery*, 2022. URL <https://openreview.net/forum?id=OdXKRtg1OG>.
- Hannes Stärk, Dominique Beaini, Gabriele Corso, Prudencio Tossou, Christian Dallago, Stephan Günnemann, and Pietro Liò. 3d infomax improves gns for molecular property prediction. In *International Conference on Machine Learning*, pp. 20479–20502. PMLR, 2022.
- Jian Tang, Meng Qu, Mingzhe Wang, Ming Zhang, Jun Yan, and Qiaozhu Mei. Line: Large-scale information network embedding. In *Proceedings of the 24th international conference on world wide web*, pp. 1067–1077, 2015.
- Jing Tang, Agnieszka Sz wajda, Sushil Shakyawar, Tao Xu, Petteri Hintsanen, Krister Wennerberg, and Tero Aittokallio. Making sense of large-scale kinase inhibitor bioactivity data sets: a comparative and integrative analysis. *Journal of Chemical Information and Modeling*, 54(3):735–743, 2014.
- Jake Topping, Francesco Di Giovanni, Benjamin Paul Chamberlain, Xiaowen Dong, and Michael M. Bronstein. Understanding over-squashing and bottlenecks on graphs via curvature. In *International Conference on Learning Representations*, 2022. URL <https://openreview.net/forum?id=7UmjRGzp-A>.
- Laurens Van der Maaten and Geoffrey Hinton. Visualizing data using t-sne. *Journal of machine learning research*, 9(11), 2008.
- Ashish Vaswani, Noam Shazeer, Niki Parmar, Jakob Uszkoreit, Llion Jones, Aidan N Gomez, Łukasz Kaiser, and Illia Polosukhin. Attention is all you need. *Advances in neural information processing systems*, 30, 2017.
- Sheng Wang, Yuzhi Guo, Yuhong Wang, Hongmao Sun, and Junzhou Huang. Smiles-bert: large scale unsupervised pre-training for molecular property prediction. In *Proceedings of the 10th ACM international conference on bioinformatics, computational biology and health informatics*, pp. 429–436, 2019.
- Yuyang Wang, Rishikesh Magar, Chen Liang, and Amir Barati Farimani. Improving molecular contrastive learning via faulty negative mitigation and decomposed fragment contrast. *Journal of Chemical Information and Modeling*, 2022a.
- Yuyang Wang, Jianren Wang, Zhonglin Cao, and Amir Barati Farimani. Molecular contrastive learning of representations via graph neural networks. *Nature Machine Intelligence*, 4(3):279–287, 2022b.
- David Weininger. Smiles, a chemical language and information system. 1. introduction to methodology and encoding rules. *Journal of chemical information and computer sciences*, 28(1):31–36, 1988.

- Zhenqin Wu, Bharath Ramsundar, Evan N Feinberg, Joseph Gomes, Caleb Geniesse, Aneesh S Pappu, Karl Leswing, and Vijay Pande. Moleculenet: a benchmark for molecular machine learning. *Chemical science*, 9(2):513–530, 2018.
- Minghao Xu, Hang Wang, Bingbing Ni, Hongyu Guo, and Jian Tang. Self-supervised graph-level representation learning with local and global structure. In *International Conference on Machine Learning*, pp. 11548–11558. PMLR, 2021.
- Dongyu Xue, Han Zhang, Dongling Xiao, Yukang Gong, Guohui Chuai, Yu Sun, Hao Tian, Hua Wu, Yukun Li, and Qi Liu. X-mol: large-scale pre-training for molecular understanding and diverse molecular analysis. *bioRxiv*, pp. 2020–12, 2021.
- Sheheryar Zaidi, Michael Schaarschmidt, James Martens, Hyunjik Kim, Yee Whye Teh, Alvaro Sanchez-Gonzalez, Peter Battaglia, Razvan Pascanu, and Jonathan Godwin. Pre-training via denoising for molecular property prediction. *arXiv preprint arXiv:2206.00133*, 2022.
- Zaixi Zhang, Qi Liu, Hao Wang, Chengqiang Lu, and Chee-Kong Lee. Motif-based graph self-supervised learning for molecular property prediction. *Advances in Neural Information Processing Systems*, 34:15870–15882, 2021.
- Gengmo Zhou, Zhifeng Gao, Qiankun Ding, Hang Zheng, Hongteng Xu, Zhewei Wei, Linfeng Zhang, and Guolin Ke. Uni-mol: A universal 3d molecular representation learning framework. 2022.
- Jinhua Zhu, Yingce Xia, Lijun Wu, Di He, Tao Qin, Wengang Zhou, Houqiang Li, and Tieyan Liu. Incorporating bert into neural machine translation. In *International Conference on Learning Representations*, 2020. URL <https://openreview.net/forum?id=Hyl7ygStwB>.
- Jinhua Zhu, Yingce Xia, Tao Qin, Wengang Zhou, Houqiang Li, and Tie-Yan Liu. Dual-view molecule pre-training. *arXiv preprint arXiv:2106.10234*, 2021.
- Yanqiao Zhu, Dingshuo Chen, Yuanqi Du, Yingze Wang, Qiang Liu, and Shu Wu. Improving molecular pretraining with complementary featurizations. *arXiv preprint arXiv:2209.15101*, 2022.